Solitary propagation effect of a well-defined chirped femtosecond laser pulse in a resonance-absorbing medium

Q. Q. Xu(许倩倩),[1] D. Z. Yao (姚端正),[1,2,*] X. N. Liu (刘晓娜),[1] Q. Zhou (周勤),[1] and G. G. Xiong (熊贵光)[1,2]

[1]*Department of Physics, Wuhan University, Wuhan 430072, China*

[2]*Key Laboratory of Acoustic and Photonics Material and Devices, Ministry of Education, Wuhan University, Wuhan 430072, China*

(Received 29 February 2012; published 29 August 2012)

We investigate the solitary propagation effect of a well-defined chirped femtosecond laser pulse in a resonance-absorbing medium which is modeled by a two-level quantum dot ensemble. Employing full time-dependent and space-dependent Maxwell-Bloch equations, the evolution of the pulse and the population inversion as well as the spectrum are obtained. The results reveal that the special chirped pulse can retain its shape and resist breakup while propagating through the absorbing medium. Besides, the spectrum does not exhibit obvious broadening but the central and near-central frequency components tend to vanish. Moreover, the stable soliton formed by the special chirped-pulse design based on stimulated Raman adiabatic passage does not obey the area theorem.

DOI: 10.1103/PhysRevA.86.023853 PACS number(s): 42.50.Gy, 42.50.Md

I. INTRODUCTION

Self-induced transparency (SIT) is an effective method of obtaining a solitary pulse induced by strong nonlinear interaction between an optical pulse and an absorbing medium. It has been widely proved in theory and experiment that an incident optical field with an even number times of π can propagate transparently without suffering absorption, but a pulse with an initial pulse area of more than 3π will split into several 2π pulses [1–5]. The potential mechanism of SIT is the area theorem controlled by the Rabi frequency, which governs the population inversion between energy levels. During past years, a robust method called stimulated Raman adiabatic passage (STIRAP), which can manage the population inversion transferred to any selected quantum state, has attracted a lot of attention and gotten fast development in theory and experiment [6–12]. In general, two sequential pulses are used in STIRAP to obtain complete population inversion by building dark states. However, this amazing process can even be accomplished by various specially designed chirped pulses [13–15]. Wang *et al*. have deduced the efficient and stable coherent population transfer in a three-level atomic medium using a superposition of two chirped Gaussian pulses with the same size but opposite sign of the chirp coefficient [16]. Torosov and co-workers also presented the imperfect population inversion to any desired state by composite sequences of frequency-chirped pulses with well-defined relative phases [17]. It is worth noticing that the effective population transfer caused by a single frequency-chirped pulse has been proved by Zhdanovich and co-workers theoretically and experimentally [18]. They achieved complete and robust population transfer to the target state by properly adjusting the amplitudes and phases of the pulses in the single-pulse train. Recently, a type of optical pulse, called the hyperbolic-square-hyperbolic pulse, was designed by Tian *et al*. for efficient uniform transparency and inversion of inhomogeneously broadened atomic ensembles [19]. These schemes expedite this method to obtain a solitary pulse in an absorbing medium, such as adiabatic self-induced transparency (ASIT) which has been offered by Loiko *et al*. to achieve a transparent pulse in a near-resonant medium [20]. The essence of ASIT is the formation of a double STIRAP by designing a special chirped pulse based on STIRAP theory, if the optical field envelope and the temporal frequency detuning of the chirped pulse can be regarded as two quasipulses. Thus, the ASIT process can avoid the adverse effect of damping from the upper state in times shorter than the relaxation time. However, although many studies pay attention to population transfer caused by several kinds of chirped pulse via STIRAP or the solitarylike ultrashort pulse propagation [21–23], there are few studies on the solitary propagation effect of this well-defined chirped pulse in an absorbing medium.

In this paper, we investigate the propagation effect of a well-defined chirped femtosecond laser pulse designed in Ref. [20] in a resonance-absorbing medium which is modeled by a two-level quantum dot ensemble. Employing full time-dependent and space-dependent Maxwell-Bloch equations, the propagation characteristics of the special chirped Gaussian pulse are explored, such as pulse profile, population inversion, and frequency spectrum, as well as pulse area. It has been found that the solitary propagation characteristics of this well-defined chirped pulse are different from the standard Gaussian pulse and also different from other kinds of chirped pulses.

II. THEORY

The model we considered is an x-polarized optical pulse propagated along the z direction from free-space into a two-level quantum dot (QD) ensemble. The one-dimensional Maxwell's equations can be written as

$$\partial_t H_y = -\frac{1}{\mu}\partial_z E_x, \tag{1}$$

$$\partial_t E_x = -\frac{1}{\varepsilon}\partial_z H_y - \frac{1}{\varepsilon}\partial_t P_x, \tag{2}$$

where E_x and H_y are the x-polarized electric field and y-polarized magnetic field, respectively. μ and ε are the permeability and permittivity of the host material. The macroscopic nonlinear polarization is represented by $P_x = N\mu_{x0}(\rho_{x0} + \rho_{0x})$, where N is the density of quantum dots, and μ_{x0} the transition dipole moment coupling two quantum

*dzyao@whu.edu.cn

states. ρ_{x0} and ρ_{0x} are the off-diagonal elements of the density matrix. In this work, we choose the exciton state $|x\rangle$ and vacuum state $|0\rangle$ of GaN-AlN quantum dot as the two-level system. The eigenstate and associated wave function as well as the transition dipole moment, which relate to the size of the QDs, are obtained through the matrix diagonalization method [24,25]. While considering an inhomogeneously broadened system, e.g., a self-assembled quantum dot ensemble, the eigenfrequency and the transition dipole moment are broadened to different extents with the size fluctuation. Therefore the macroscopic nonlinear polarization can be denoted as a summation of all the fractional polarization resulting from diverse detuning simultaneously [26]. That is, $P_x = \sum_m P_{m,x} = \sum_m N_m \mu_{m,x0}(\rho_{m,x0} + \rho_{m,0x})$. N_m is the density of quantum dots at the mth eigenfrequency and $N = \sum_m N_m$.

Beyond the rotation wave approximation and the slowly varying envelope approximation, the optical Bloch equations can be written as [26]

$$\partial_t u = -\frac{1}{T_2}u + \omega_{x0}v, \tag{3}$$

$$\partial_t v = -\omega_{x0}u - \frac{1}{T_2}v + 2\Omega w, \tag{4}$$

$$\partial_t w = -2\Omega v - \frac{1}{T_1}(w - w_0), \tag{5}$$

where $u = \rho_{x0} + \rho_{0x}$, $v = i(\rho_{x0} - \rho_{0x})$, and $w = \rho_{xx} - \rho_{00}$, with ρ_{xx} and ρ_{00} being the diagonal elements of the density matrix. ω_{x0} is the eigenfrequency of the two-level system, and $\Omega = E_x \mu_{x0}/\hbar$ the Rabi frequency. T_1 and T_2 are the longitudinal relaxation time and transverse relaxation time, respectively. The three components u, v, and w of the Bloch equations also relate to the dispersion properties of the transition process, the absorption of input pulse by the medium, and the population transfer of the two-level system, respectively.

If there is a source field in the space at any moment, the distribution of the electric field and magnetic field as well as the response of the medium at any time later can be obtained by solving the Maxwell-Bloch equations (1)–(5). We assume the resonant two-level system is at the ground state ($w_0 = -1$) and $u = v = 0$ initially. The input pulse exhibits a Gaussian profile,

$$E_x(z=0,t) = E_0 \exp\left[-\frac{(t-t_0)^2}{T_\Omega^2}\right]\cos\{[\omega_{x0} + \omega(t-t_0)]t\}, \tag{6}$$

where E_0 is the maximum amplitude of the electric field, T_Ω the pulse duration, and t_0 is chosen for keeping the pulse outside the computational domain at $t = 0$. The pulse area of the Gaussian profile is defined as $A = \sqrt{\pi}\Omega T_\Omega$. To manifest the dissimilar performance of the special chirped pulse designed in Ref. [20], two cases are considered in this paper. One is $\omega(t) = 0$, where the input pulse is a standard Gaussian pulse with carrier frequency ω_{x0}. The other one is the well-defined chirped pulse with $\omega(t) = \Omega\{\exp[-(t-\Delta_T)^2/T_\Omega^2] + \exp[-(t+\Delta_T)^2/T_\Omega^2]\}$, which is built according to the ASIT theory based on a double-STIRAP process. Then, the Maxwell-Bloch equations can be solved effectively by an iterative predictor-corrector finite-difference time-domain method [23,27]. In this paper,

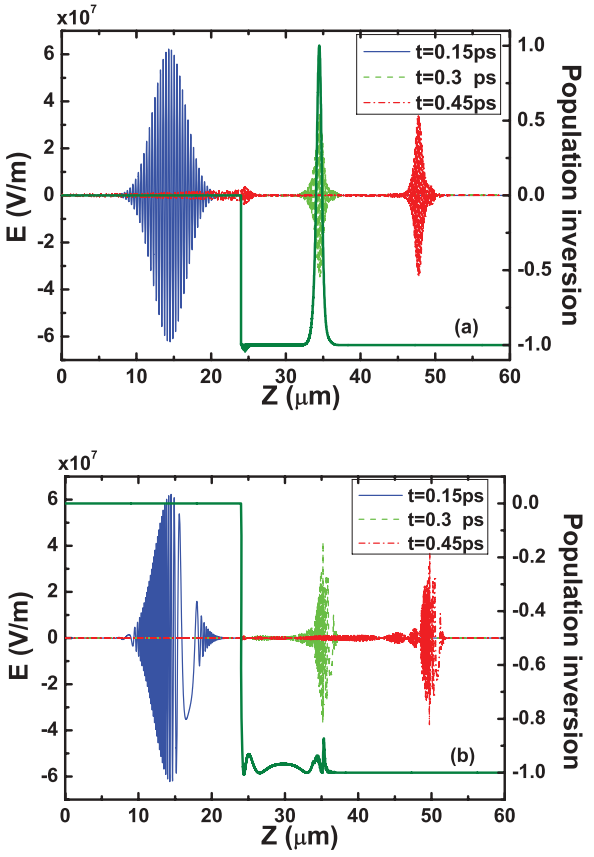

FIG. 1. (Color online) The snap of the electric field with 4π area propagating in an absorbing medium with $\varepsilon_r = 9.5$ at $t = 0.15$, 0.3, and 0.45 ps. The population inversion at 0.3 ps. (a) Standard field; (b) special chirped field.

the radius of the core-shell GaN-AlN QD is considered as 4.3 nm (the core) and the thickness of the shell is 1.5 nm. We obtain the eigenfrequency and transition dipole moment related to this size as $\omega_{x0} = 5.1 \times 10^{15}$ rad/s and $\mu_{x0} = 1.1 \times 10^{-27}$ C m, respectively. The other parameters involved are the following unless there is a special statement: $N = 8 \times 10^{21}$ m^{-3}, $T_1 = 120$ ps, $T_2 = 80$ ps, the relative index $\varepsilon_r = 9.5$, $\Delta_T = 1.5T_\Omega$, $t_0 = 10T_\Omega$, and the full width at half maxima (FWHM) of the pulse $t_p = 12$ fs.

III. RESULTS AND DISCUSSIONS

We suppose the GaN-AlN QD ensemble is placed in the vacuum and the left side is at $z = 24$ μm. The pulse source is located at $z = 0$ μm. To begin with, we investigate the propagation characteristics of a 4π standard and the well-defined chirped Gaussian pulse from vacuum space injected into the two-level absorption system. Figures 1(a) and 1(b) each exhibit the snapshot of the standard pulse and the tailored pulse at 0.15, 0.3, and 0.45 ps. It is obvious that both of the pulses have not been injected into the medium when $t = 0.15$ ps, therefore they exhibit the initial complete pulses at that time. Later on, the pulses enter into the absorption medium and almost half reflection happens at the incident face. The amplitude of the pulses drops to half of the initial amplitude and propagates more slowly than in vacuum. A

detailed description follows: we first analyze the propagation of the standard pulse in Fig. 1(a). Comparing the shape of the pulse at the three considered time, it is obvious to find that the pulse suffers serious distortion at the front side of the pulse and slight distortion at the end. The strong distortion of the front side is ascribed to the beginning of the pulse splitting, while the slight distortion of the end side is confirmed due to the reshaping of the pulse caused by the combined effect of self-phase modulation and group velocity dispersion [28]. The same effect also appears in Fig. 1(b), the evolution of the well-defined chirped pulse, but conversely, large distortion presents at the end side of the chirped pulse and there is no distortion at the front. This means there will be no pulse splitting along the propagation of the well-defined chirped pulse. Then, the population inversions in the absorption medium, each aroused by the two different pulses, are explored. The thick lines in Figs. 1(a) and 1(b) depict the population inversions at 0.3 ps. For the case of the standard pulse, population inversion happens at the front half of the pulse and the complete inversion emerges at the peak of the pulse and subsequently declines rapidly at the second half of the pulse. The process is typically the traditional self-induced transparency, expressed as an energy absorption during the front half of pulse and a stimulated emission during the second half (i.e., the slow light effect). But in the case of the special chirped pulse, the behavior of population inversion related to the pulse is tremendously different. As shown in Fig. 1(b), a slight inversion appears at the front of pulse and then forms a series of oscillations and at last locates in the range from -0.9 to -1. This is because as the single STIRAP can stimulate the complete inversion powerfully, the double STIRAP caused by the well-defined chirped pulse can create the second inversion before the first complete inversion. Therefore, the whole effect of the double STIRAP is the strong restraint of the population inversion. It means that the pulse can propagate through the absorbing medium without absorption and thus avoids the damping effects, such as the unexpected spontaneous emission from the upper state during the time that is shorter than the relaxation time. Additionally, unlike the slow light effect of the standard pulse, the velocity of the special chirped pulse is a little faster owing to the fact that its propagating process almost does not involve the energy transfer between the pulse and the medium.

Due to the fact that dot-size fluctuation always appears in a self-assembled QD ensemble, we consider that the special chirped pulse transmits in an inhomogeneously broadened medium with the full width at half maxima (σ_{FWHM}) of 25 meV. The eigenfrequency ω_{x0} of the medium is not a uniform constant anymore but is center spread into a Gaussian distribution $G(\omega_{m,x0}) = 1/\sqrt{2\pi}\sigma \exp[-(\omega_{m,x0} - \omega_{x0})^2/2\sigma^2]$ [5], where $\sigma_{\mathrm{FWHM}} = 2\sigma\sqrt{2\ln 2}$. These broadened frequencies form various detunings from the central frequency $\delta = \omega_{m,x0} - \omega_{x0}$. We gain the different eigenfrequencies $\omega_{m,x0}$ and transition dipole moments $\mu_{m,x0}$ in the same way as ω_{x0} and μ_{x0} within different radius sizes. Then, each fractional polarization $P_{m,x}$ can be obtained through Eqs. (3)–(5) by replacing ω_{x0} and μ_{x0} with $\omega_{m,x0}$ and $\mu_{m,x0}$, respectively. In our calculation, we define $m = 1,2,\ldots,500$. As depicted in Fig. 2(a), the shape of the pulse at 0.3 ps is similar to the initial input pulse, but a sharp gradient appears at the end of the pulse when the time comes to 0.45 ps. Comparing to Fig. 1(b), it is easy to draw the conclusion that the influence of pulse reshape is weak while considering the effect of inhomogeneous broadening. In addition, the population inversions related to the special chirped pulse at 0.49 ps are shown in Fig. 2(b). For convenience, only the evolution of population inversions of three representative detunings are shown. It is clear to see that while the frequency of the pulse first drops, the population inversions of various detunings rise to different values and then oscillate strongly when the frequency of the pulse increases. Finally, they form a stable location which is monotonous related to the detuning. For the case of $\delta < 0$, i.e., in those QDs that have radii larger than the average radius, the population inversions stabilize at a range from -0.45 to 0.35, and at a range from -0.45 to -0.65 for the case of $\delta > 0$, meaning in those smaller QDs. To explain this marvelous phenomenon, we can quote the STIRAP theory by denoting the special chirped pulse as two quasipulses: One is the Δ quasipulse formed from the detuning between transient frequencies of the chirped pulse and the different eigenfrequencies of the QDs, i.e., $\Delta(\delta,t) = \omega_{x0} + \omega(t) - \omega_{m,x0} = \omega(t) - \delta$; the other is the Ω quasipulse formed from transient Rabi frequencies, i.e., $\Omega(\delta,t) = \Omega_m \exp[-(t - t_0)^2/T_\Omega^2]$, where $\Omega_m = E_x\mu_{m,x0}/\hbar$. As known, smaller QDs have a higher eigenenergy and slightly lower transition dipole moment than the average value [29].

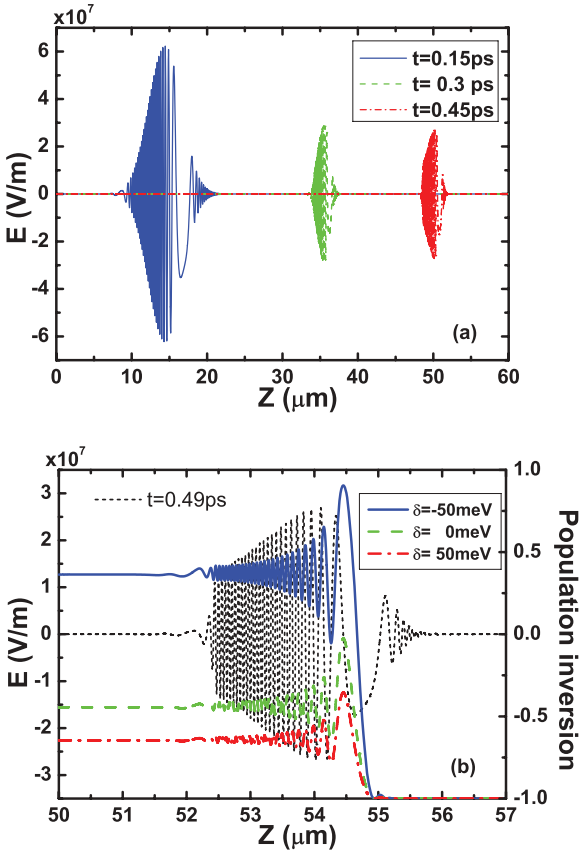

FIG. 2. (Color online) (a) The snap of the special chirped pulse with 4π area propagating in an inhomogeneously broadened absorbing medium with $\varepsilon_r = 9.5$ at $t = 0.15$, 0.3, and 0.45 ps. (b) The population inversion of the three detunings at 0.49 ps.

Therefore even the Ω quasipulse is slightly weak; the increasing of the Δ quasipulse also enhances the formation of adiabatic passage. On the other hand, larger QDs possess lower eigenenergies and slightly higher transition dipole moments. Thus, the decrease of the Δ quasipulse causes the dramatically decreasing Δ pulse area, and the difference in the area of the two transient quasipulses is notably increased under this case. According to STIRAP theory, the formation of an adiabatic passage will be conspicuously destroyed. Hence, the propagation of the special chirped pulse in large QDs tends slightly toward SIT. Due to the fact that the sizes of most QDs are nearly identical with the average size, therefore, the well-defined chirped pulse also can propagate solitarily in an inhomogeneously broadened medium losing less energy.

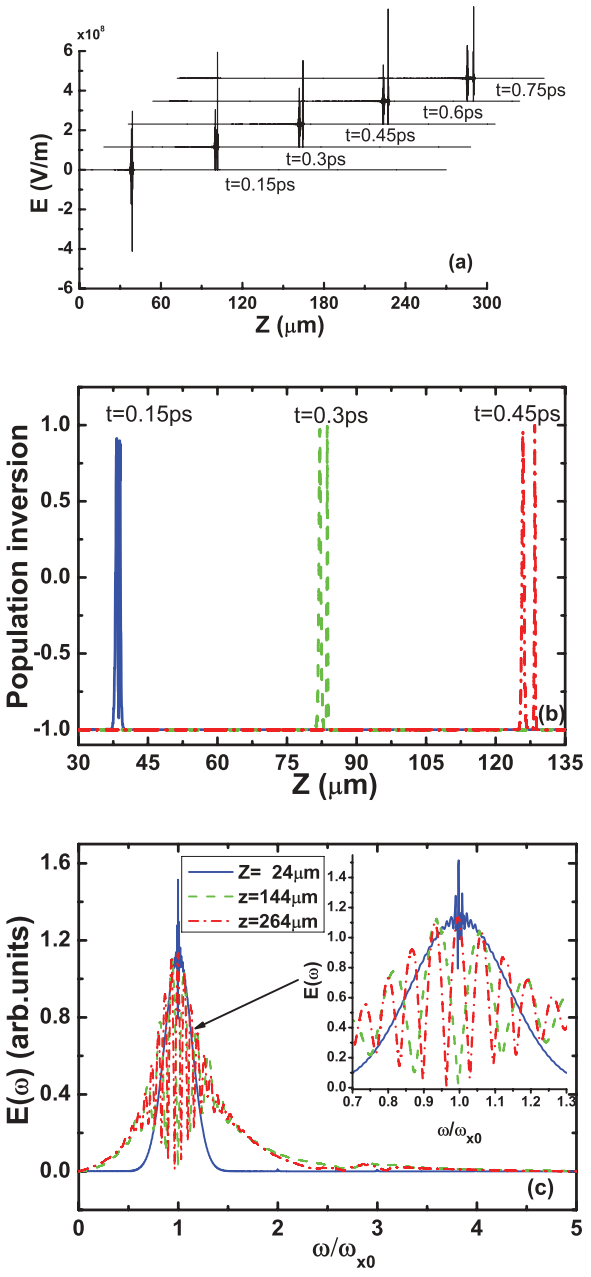

FIG. 3. (Color online) (a) The propagation of the standard pulse with 4π area propagating in an absorbing medium with $\varepsilon_r = 1$, $t_p = 2.4$ fs at five different times. (b) The population inversion at $t = 0.15$, 0.3, and 0.45 ps. (c) The frequency spectrum of the pulse at $Z = 24$, 144, and 264 μm.

As follows, the propagation characters such as the splitting effect and the spectral character of the standard pulse and the special chirped pulse are investigated. Obviously, the parameters we used in Figs. 1 and 2 cannot provide such long research time and distance. For exploring the long transmission effect with less amount of calculation, we study a short 4π pulse ($t_p = 2.4$ fs) propagating in a two-level absorption system with nonrealistic relative index $\varepsilon_r = 1$. The changing of the two parameters causes no loss of effectiveness of the propagation properties such as the shape of the pulse and the spectrum in which we are interested [30,31]. The propagation characters of the two different pulses are shown in Figs. 3 and 4, respectively. As shown in Fig. 3(a), the standard pulse injects into the medium before 0.15 ps and gradually splits into two nonidentical pulses with different amplitude and velocity. The fast one is more intense and a little shorter than the other. Figure 3(b) clearly depicts the evolution of population inversion caused by the standard pulse. As the pulse splits, the population transfer makes two complete inversions so it is easy to draw the conclusion that the pulse areas of the two nonidentical pulses are 2π. Moreover, the spectrum characteristic of the propagating pulse is an important factor to measure the solitary propagation effect [21]. Figure 3(c) shows the frequency spectrum at 24, 144, and 264 μm. At the left side of the medium, the spectrum exhibits a narrow range from $0.6\omega_{x0}$ to $1.4\omega_{x0}$. With the long propagation, the spectrum extended dramatically, especially at the higher spectral side. Evidently, strong oscillation of the spectrum appears near the central frequency and becomes stronger as the pulse propagates. The inset in Fig. 3(c) exhibits the detailed part of the oscillation and a nonmonotonous change is demonstrated at the central frequency. However, the width of the spectrum does not vary notably and presents a nonmonotonous change with propagation distance. This abnormal feature of a standard Gaussian pulse is consistent with the property of a hyperbolic secant pulse, which is discussed in detail in Ref. [30].

Figure 4(a) shows the propagation effect of the special chirped pulse transmissions under the same circumstance. Unlike the propagation of a standard pulse, no split appears when this well-defined chirped pulse propagates, and the pulse shape can be retained along the propagation. This result is also radically different from that of Ref. [28]; the authors of that work adopt a combined general chirped pulse which is different from our method. The reason is that the propagation of the well-defined chirped pulse based on STIRAP does not suffer absorption and stimulated emission governed by the Rabi flopping. The evolution of population inversion shown in Fig. 4(b) also supports the explanation. As discussed above, the maximum inversion is achieved to a low value and the line exhibits no intention to split. It is essential to note that the value of the maximum inversion is largely higher and the amplitude of residual fluctuation is obviously weaker than that in Fig. 1(b). This phenomenon reveals that increasing the amplitude of the pulse can enhance the role of STIRAP and form a stronger transparent signal. Different from the spectrum of a standard pulse in Fig. 3(c), the spectrum of the special chirped pulse depicted in Fig. 4(c) exhibits a

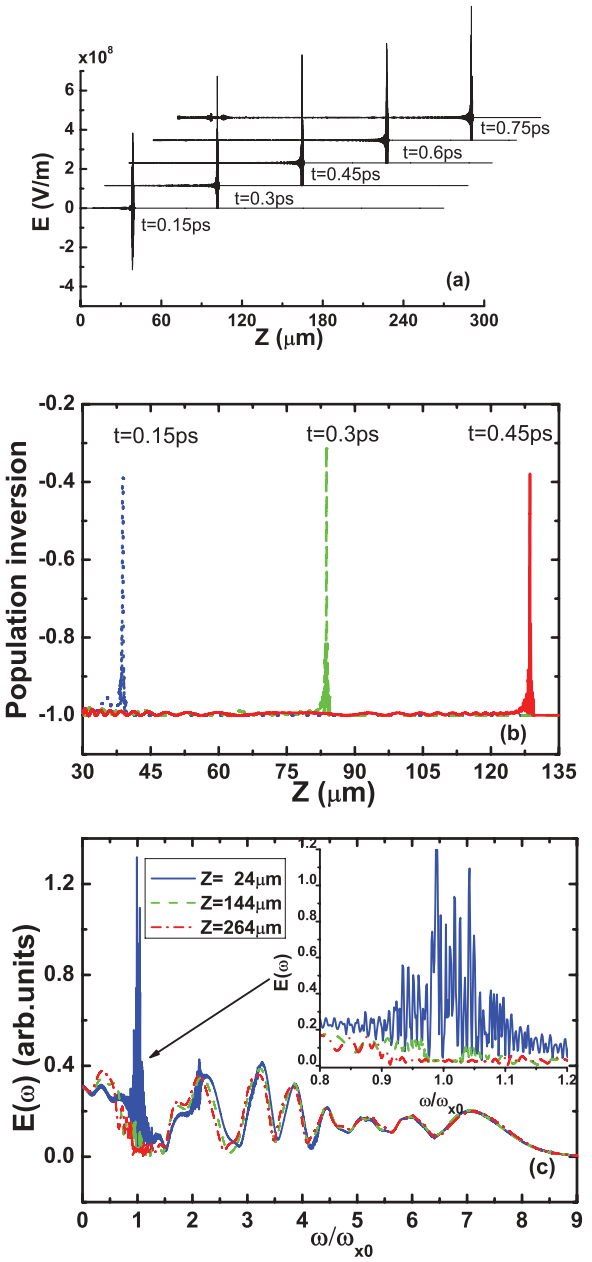

FIG. 4. (Color online) (a) The propagation of the special chirped pulse with 4π area propagating in an absorbing medium with $\varepsilon_r = 1$, $t_p = 2.4$ fs at five different times. (b) The population inversion at $t = 0.15$, 0.3, and 0.45 ps. (c) The frequency spectrum of the pulse at $Z = 24$, 144, and 264 μm.

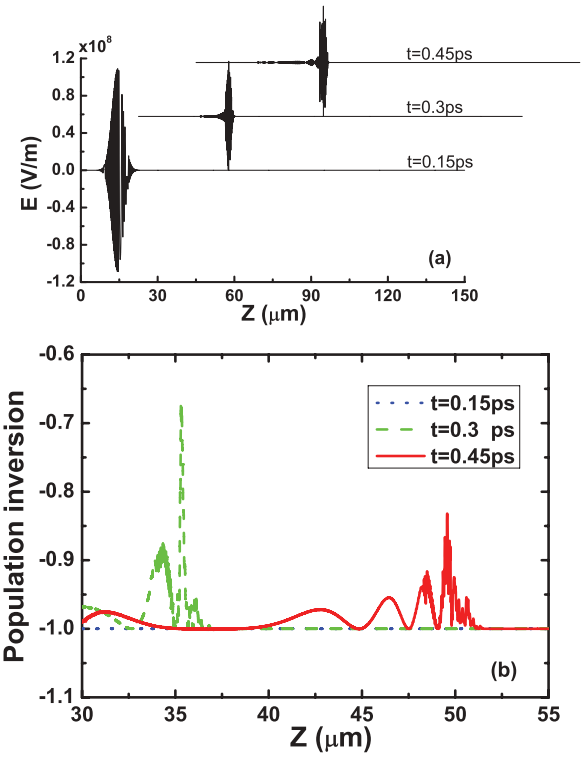

FIG. 5. (Color online) (a) The propagation of the special chirped pulse with 7π area propagating in an absorbing medium with $\varepsilon_r = 9.5$ at $t = 0.15$, 0.3, and 0.45 ps. (b) The population inversion at 0.15, 0.3, and 0.45 ps.

quite broad width in the range from 0 to $9\omega_{x0}$ due to the designed chirp described in Sec. II. Obviously, there are more higher-frequency components than lower and all of them form relaxed fluctuations. As the pulse propagates, the width of the spectrum does not show notable extension and the distribution changes slightly at higher frequencies from $4\omega_{x0}$ to $9\omega_{x0}$. Moreover, the spectral components among 0 to $4\omega_{x0}$ shift to the central frequency a little, and the components at and near the central frequency diminish quickly and even vanish at last. All in all, the tailored pulse can propagate in a pulse-preserving way and scarcely spur population inversion in a resonant medium. Besides, the almost unchanged spectrum (except the components of central and near-central frequency) further demonstrates that solitary behavior can be retained over a long distance.

Finally, we investigate the effect of an odd number of pulse areas on the propagation of the special chirped pulse. Generally speaking, a particular trait of SIT is the breakup of a pulse with an area above 3π into 2π pulses with different amplitudes and different group velocities. Therefore the extra pulse area less than π will be absorbed while it propagates, which is named as self-induced absorption. However, as seen in Fig. 5(a), the pulse with 7π and $t_p = 12$ fs also propagates like a soliton without losing energy in the absorbing medium with $\varepsilon_r = 9.5$. That means that the propagation of this special chirped pulse design based on STIRAP does not obey the area theorem, as discussed in Ref. [20]. Nevertheless, it must depend on the adiabatic condition. According to the theory of STIRAP, the two sequential quasipulses derived from the special chirped pulse can form dark states in the medium. One of them is $\Phi_-(t) = |0\rangle \cos\Theta(t) - |x\rangle \sin\Theta(t)$, with $\Theta(t) = \arctan[\Omega(t)/\Delta(t)]$ being the mixing angle and the adiabatic condition can be described as $\sqrt{\Omega^2(t) + \Delta^2(t)} \gg |\dot{\Theta}(t)|$ [10]. Therefore, the well-defined chirped pulse will make a better performance with a larger pulse area. Generally speaking, the low threshold is 4π [20]. The related population inversion depicted in Fig. 5(b) appears less different from the inversion aroused by a 4π pulse in Fig. 1(b), except for a little high value of the maximum inversion and the smaller amplitude of the residual fluctuation. This result supports the STIRAP theory that the larger the pulse area, the better the transparent

signal. The investigations related to pulse area reveal that the solitary behavior of the tailored pulse does not depend on the area theorem, but is dominated by adiabatic conditions. So the solitary propagation effect of the well-defined pulse cannot happen, and the area theorem also governs the interaction process of the pulse and medium if the pulse area is quite small.

IV. CONCLUSION

We have investigated the propagation of a standard pulse and a well-defined chirped pulse in a two-level system by solving the full Maxwell-Bloch equations using an iterative predictor-corrector finite-difference time-domain method. The results demonstrate that the special chirped pulse design based on STIRAP can retain its shape and resist breakup as it does not experience absorption or refraction while propagating through the absorbing medium. Besides, unlike the spectral broadening of the standard pulse, the frequency spectrum width of the special chirped pulse does not exhibit obvious changing. However, the central frequency and near-central frequency components of the special chirped pulse diminish quickly and even vanish as they are propagating. Furthermore, these characteristics also can be sustained while for the special chirped pulse with an odd number of pulse areas, which demonstrate the disagreement with area theorem of the pulse. To sum up, the well-defined chirped pulse possesses outstanding capability to form stable solitons without strictly following the area theorem.

ACKNOWLEDGMENTS

This work was financially supported by the National Natural Science Foundation of China under Grant No. 10534080.

[1] B. Macke and B. Séard, Phys. Rev. A **81**, 015803 (2010).
[2] A. Skryabin, Opt. Express **16**, 4858 (2008).
[3] Q. Dai, H. Liu, J. Liu, L. Wu, Q. Guo, W. Hu, X. Yang, S. Liu, S. Lan, and A. Gopal, Appl. Phys. Lett. **92**, 153111 (2008).
[4] N. Cui, Y. Niu, H. Sun, and S. Gong, Phys. Rev. B **78**, 75323 (2008).
[5] G. Panzarini, U. Hohenester, and E. Molinari, Phys. Rev. B **65**, 165322 (2002).
[6] T. Rickes, L. Yatsenko, S. Steuerwald, T. Halfmann, B. Shore, N. Vitanov, and K. Bergmann, J. Chem. Phys. **113**, 534 (2000).
[7] N. Vitanov, T. Halfmann, B. Shore, and K. Bergmann, Annu. Rev. Phys. Chem. **52**, 763 (2001).
[8] A. D. Greentree, J. H. Cole, A. R. Hamilton, and L. C. L. Hollenberg, Phys. Rev. B **70**, 235317 (2004).
[9] H. Goto and K. Ichimura, Phys. Rev. A **74**, 053410 (2006).
[10] N. Vitanov and B. Shore, Phys. Rev. A **73**, 053402 (2006).
[11] J. Klein, F. Beil, and T. Halfmann, Phys. Rev. A **78**, 033416 (2008).
[12] E. R. Schmidgall, P. R. Eastham, and R. T. Phillips, Phys. Rev. B **81**, 195306 (2010).
[13] H. Y. Hui and R. B. Liu, Phys. Rev. B **78**, 155315 (2008).
[14] B. Fainberg and V. Gorbunov, J. Chem. Phys. **117**, 7222 (2002).
[15] C. M. Simon, T. Belhadj, B. Chatel, T. Amand, P. Renucci, A. Lemaitre, O. Krebs, P. A. Dalgarno, R. J. Warburton, X. Marie, and B. Urbaszek, Phys. Rev. Lett. **106**, 166801 (2011).
[16] Z. Wang, K. Jia, Y. Liang, D. Tong, and X. Fan, Proc. SPIE **7846**, 78460M (2010).
[17] B. T. Torosov, S. Guérin, and N. V. Vitanov, Phys. Rev. Lett. **106**, 233001 (2011).
[18] S. Zhdanovich, E. A. Shapiro, M. Shapiro, J. W. Hepburn, and V. Milner, Phys. Rev. Lett. **100**, 103004 (2008).
[19] M. Tian, T. Chang, K. D. Merkel, and W. R. Babbitt, Appl. Opt. **50**, 6548 (2011).
[20] Y. Loiko, C. Serrat, R. Vilaseca, V. Ahufinger, J. Mompart, and R. Corbalán, Phys. Rev. A **79**, 053809 (2009).
[21] V. P. Kalosha and J. Herrmann, Phys. Rev. Lett. **83**, 544 (1999).
[22] Y. Y. Lin, I. H. Chen, and R. K. Lee, Phys. Rev. A **83**, 043828 (2011).
[23] A. Pusch, J. M. Hamm, and O. Hess, Phys. Rev. A **84**, 023827 (2011).
[24] S. Kim, S. Hong, and K. Yeon, Phys. Rev. B **76**, 115322 (2007).
[25] Y. Hu, M. Lindberg, and S. Koch, Phys. Rev. B **42**, 1713 (1990).
[26] F. Schlottau, M. Piket-May, and K. Wagner, Opt. Express **13**, 182 (2005).
[27] R. W. Ziolkowski, J. M. Arnold, and D. M. Gogny, Phys. Rev. A **52**, 3082 (1995).
[28] Z. Wang, Z. Liu, Y. Liang, K. Jia, and X. Fan, Proc. SPIE **7846**, 78460R (2010).
[29] L. Liu, J. Li, and G. Xiong, Physica E **25**, 466 (2005).
[30] R. Zhang, D. Yao, Q. Xu, and X. Liu, Eur. Phys. J. B **84**, 161 (2011).
[31] K. Xia, S. Gong, C. Liu, X. Song, and Y. Niu, Opt. Express **13**, 5913 (2005).